The spatial receptive field of thalamic inputs to single cortical simple cells revealed by the interaction of visual and electrical stimulation

Prakash Kara*, John S. Pezaris, Sergey Yurgenson, and R. Clay Reid

Department of Neurobiology, Harvard Medical School, Boston, MA 02115

Communicated by David H. Hubel, Harvard Medical School, Boston, MA, October 15, 2002 (received for review September 9, 2002)

Electrical stimulation of the thalamus has been widely used to test for the existence of monosynaptic input to cortical neurons, typically with stimulation currents that evoke cortical spikes with high probability. We stimulated the lateral geniculate nucleus (LGN) of the thalamus and recorded monosynaptically evoked spikes from layer 4 neurons in visual cortex. We found that with moderate currents, cortical spikes were evoked with low to moderate probability and their occurrence was modulated by ongoing sensory (visual) input. Furthermore, when repeated at 8–12 Hz, electrical stimulation of the thalamic afferents caused such profound inhibition that cortical spiking activity was suppressed, aside from electrically evoked monosynaptic spikes. Visual input to layer 4 cortical cells between electrical stimuli must therefore have derived exclusively from LGN afferents. We used white-noise visual stimuli to make a 2D map of the receptive field of each cortical simple cell during repetitive electrical stimulation in the LGN. The receptive field of electrically evoked monosynaptic spikes (and thus of the thalamic input alone) was significantly elongated. Its primary subfield was comparable to that of the control receptive field, but secondary (flanking) subfields were weaker. These findings extend previous results from intracellular recordings, but also demonstrate the effectiveness of an extracellular method of measuring subthreshold afferent input to cortex.

Orientation selective neurons in primary visual cortex receive feed-forward input from lateral geniculate nucleus (LGN) cells that are themselves poorly oriented. Experiments that have examined the role of the feed-forward thalamocortical pathway in this receptive field transformation have yielded two independent findings. First, the thalamic input to cortical simple cells is highly specific; LGN cells make monosynaptic connections with simple cells predominantly when the pre- and postsynaptic receptive fields overlap and match in sign, size, and time course (1, 2). Second, when intracortical inputs are silenced by cooling or by electrical stimulation in cortex, intracellular recordings demonstrate that the summed thalamic input to a layer 4 simple cell is orientation selective (3, 4). Here, we present a technique that we have used to examine a related but hitherto untested hypothesis: that the spatial receptive field of a simple cell is very similar to the receptive field of its summed thalamic input. We have concentrated on two receptive-field parameters, the elongation of the strongest subfield and the relative strength of antagonistic, flanking subfields.

The experimental approach that we took to examine these questions was based on two independent characteristics of electrical stimulation: (*i*) if electrical stimulation is not 100% effective in evoking cortical spikes, then the probability of evoking a spike will depend on the subthreshold activity of the cortical neuron at the time of the stimulus, and (*ii*) strong electrical stimulation leads to prolonged (100–200 ms) inhibition of cortical firing (5). Reversal of this inhibition during intracellular recording and γ-aminobutyric acid (GABA) blockade (6) suggests that the inhibition is indeed intracortical, although shorter-lived inhibition is presumed to be present in the thalamus as well (see *Discussion*). With low currents, electrical stimulation of the LGN evokes cortical spikes with low probability (and thus will be strongly modulated by ongoing visual input) but feed-forward inhibition is weak. With higher currents, electrical stimulation evokes spikes with higher probability and feed-forward inhibition is strong and long lasting. The key point for the experiments reported here was that we were able to find stimulation parameters ($\approx$200 μA pulses, delivered at 8–12 Hz) such that the efficacy of each stimulus was $<$100% and cortical activity was silenced between successive stimuli. Because electrical stimuli were $<$100% effective, ongoing visual stimulation modulated their efficacy, so that the probability that a thalamocortical excitatory postsynaptic potential evoked a spike served as a readout of subthreshold visual input (Fig. 1). Further, because the cortex was silenced, all visual input must have derived from the thalamus. When combined with stimuli that map the receptive field in two dimensions (e.g., Fig. 3*A*), repetitive electrical stimulation therefore served as a tool to determine the receptive field of the summed thalamic input to a simple cell.

We found that the summed receptive field of the thalamic inputs onto individual cortical layer 4 simple cells was significantly elongated. That is, the length-to-width aspect ratio of the strongest subfield was significantly greater than 1. Subfields flanking the peak subfield, a hallmark of the receptive field of simple cells, were weaker and not always evident in the receptive field of the thalamic input. Although comparable data may be attainable with intracellular recordings, the approach used in this study has the benefit that it is based on technically simpler extracellular recordings.

Materials and Methods

Preparation and Anesthesia. Seven anesthetized, paralyzed cats (1.5–4.5 kg) were used. The presurgical preparation, induction and maintenance anesthesia, ocular stabilization, and optical refractive methods have been described (7). Surgical anesthesia was induced with ketamine HCl (10 mg/kg, i.m.) and continued with thiopental sodium (20 mg/kg, i.v., supplemented as needed). During electrophysiological recording, anesthesia was maintained with thiopental sodium (2–3 mg/kg/hr, in 0.9% saline, i.v.). Surgical and experimental procedures were in accordance with National Institutes of Health and U.S. Department of Agriculture guidelines and were approved by the Harvard Medical Area Standing Committee on Animals.

Electrophysiology, Visual and Electrical Stimulation, and Receptive Fields. We recorded extracellularly from single units along the medial bank of layer 4 of area 17 with platinum-plated tungsten-in-glass electrodes (8). We stimulated in the LGN by using a single tungsten microelectrode (AM Systems, Carlsborg, WA; 1–5 MΩ) positioned in the A lamina. Before stimulation, we

Abbreviation: LGN, lateral geniculate nucleus.

*To whom correspondence should be addressed. E-mail: pkara@hms.harvard.edu.

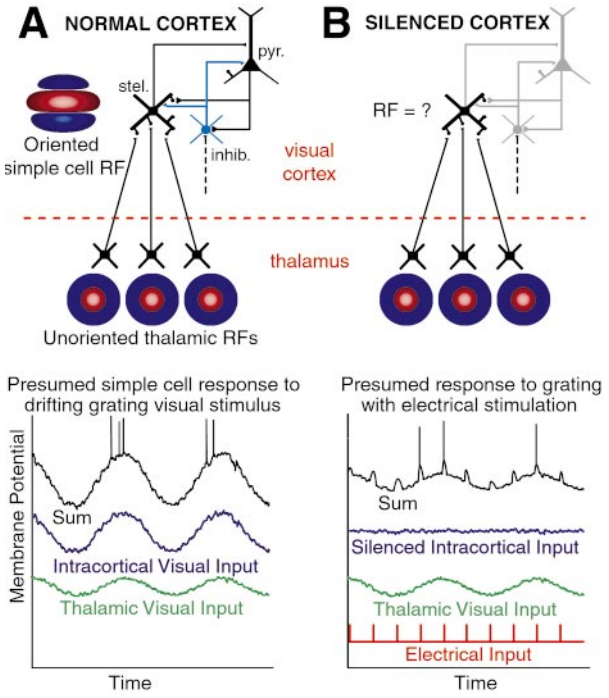

Fig. 1. Presumed thalamocortical circuit and visual responses in normal and silenced cortex. (*A Upper*) Model of thalamocortical circuit. Circular receptive fields of thalamic cells are transformed to an elongated cortical receptive field by the convergence of inputs (adapted from refs. 1 and 27). *On* subfields are shown in red, and *off* subfields are blue. In this model, recurrent intracortical connections (excitatory, from pyramidal and spiny stellate cells; and inhibitory) amplify thalamic input but are not required for generating the elongated cortical receptive field. (*Lower*) Schematic responses to a drifting sine grating stimulus, decomposed into a thalamic component (green) and a larger intracortical component (blue). At optimal phases of the visual stimulus the summed components (black) exceed threshold and induce spiking. (*B Upper*) Thalamocortical circuit when cortical spiking is silenced by feed-forward inhibition. (*Lower*) Schematic responses to visual stimulus during repetitive electrical stimulation of the LGN at a rate of 8–12 Hz (red). Electrical stimulation spares the monosynaptic visually evoked thalamic input but silences intracortical activity in the period between electrical stimuli. The result is that the cortical membrane potential remains below spiking threshold at all times except when an electrical pulse is delivered. The relative probability of electrically evoked spiking is modulated by the residual visual input from the LGN. Thus repetitive electrical stimulation serves double duty: it silences cortex and probes the visual drive from the LGN.

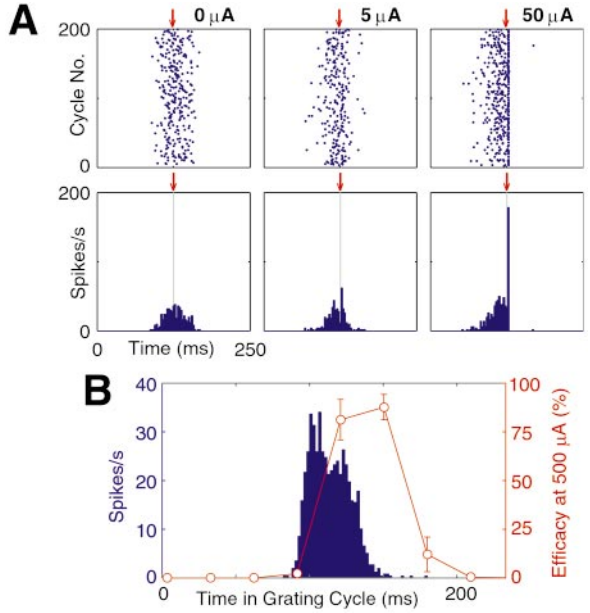

Fig. 2. Efficacy of electrical stimulation varies with stimulus current (*A*) and phase of sine grating visual stimulus (*B*). (*A*) Raster plot and PSTH from the responses of a simple cell to 200 repeats of a drifting grating visual stimulus under control conditions (0 μA) and during electrical stimulation of the LGN (5 and 50 μA). Electrical stimuli were applied close to the peak of the visual response (red arrow). Five-microampere stimulation led to a slightly higher probability (6%) of the cortical cell firing a spike within $\approx$2 ms, compared with control. This relatively weak stimulation current partially suppressed the ongoing visually evoked response. Fifty-microampere electrical stimulation of the same cell evoked monosynaptic spikes with high probability (42%) and almost completely silenced the remaining activity. PSTH bin width: 2.5 ms. (*B*) Response PSTH of a different cortical cell to a drifting sine grating stimulus (blue histogram, ordinate at left; bin width = 3 ms). Superimposed is the efficacy of electrical stimulation applied at different phases of the visual stimulus (red curve, ordinate at right). Electrical stimuli were applied every 90 ms, whereas the visual stimulus was drifted with a period of 240 ms. Thus, for every three cycles of the visual stimulus, the electrical stimulus occurred at eight distinct phases. Other than monosynaptic spikes, repetitive electrical stimulation silenced >98% of cortical activity. The efficacy of electrical stimulation in producing a cortical spike reflects the subthreshold visually evoked input from the thalamus. Error bars ($\pm$ SD) were obtained by calculating the efficacy separately for 10 equal segments of the data.

recorded multiunit activity from the LGN stimulating electrode to assess retinotopic overlap with cortical single-unit receptive fields.

Recordings were targeted to layer 4 by careful placement of the electrode relative to the medial margin of the lateral gyrus. During experiments, we confirmed that we were recording in layer 4 with the following criteria: (*i*) short-latency (1.8–2.4 ms) activation from LGN, consistent with monosynaptic activation, but without the longer latency (3.1–30 ms), high threshold and low-jitter activation typical of antidromic stimulation of layer 6 neurons (9); (*ii*) predominance of simple receptive fields; and (*iii*) presence of unoriented background "hash" caused by the high density of thalamic afferents. Histological reconstructions, done for 8 of 15 cases, confirmed that the recordings were in layer 4.

We characterized receptive fields before and during LGN electrical stimulation by presenting visual stimuli on a 21-inch computer monitor (model 817P, ViewSonic, Walnut, CA) viewed monocularly at a distance of 114 cm, with a frame rate of 170 Hz and mean luminance of 48 cd/m^2. A binary white-noise visual stimulus, updated every 29.4 ms (five video frames), was used to map receptive fields (10). Individual stimulus pixels were sized (0.4° or 0.6°) so that receptive-field subregions were 4–8 pixels long and 2–3 pixels wide.

Optimally oriented drifting sinusoidal gratings (4 Hz, 25–50% contrast) were used to test the efficacy of electrical stimulation applied at various phases of the visual response (see Fig. 2). For all cells, we first applied electrical stimuli at 2 Hz (every other cycle of the grating stimulus) close to the peak of the visually evoked grating response. This allowed us to demonstrate monosynaptic input with low stimulus current, as well as to assess feed-forward suppression for higher stimulus currents. Each monopolar cathodal stimulation pulse lasted 0.2 ms and had an intensity of 5–500 μA. Typically, 200–250 μA was effective in suppressing >95% of cortical activity for 100–200 ms after the monosynaptic spike.

Once the probability of evoking a monosynaptic spike and the extent of cortical suppression was established, we proceeded to stimulate the LGN repetitively during white-noise visual mapping or drifting grating stimuli. During white-noise visual stimulation, electrical pulses applied at every fourth or fifth frame

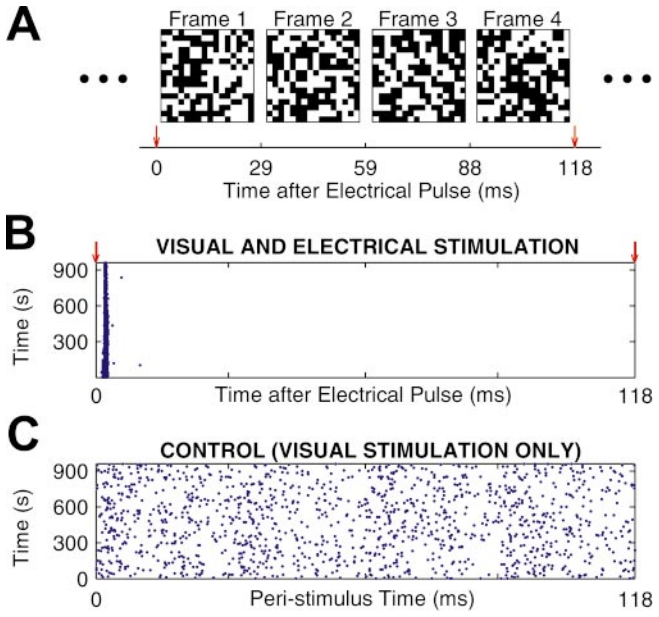

Fig. 3. Cortical response to combined white noise and electrical stimulation. (*A*) Each frame of the white-noise visual stimulus was a unique checkerboard (16 × 16 matrix) of white and black squares. Four such frames, which were presented every 29.4 ms, are shown. Electrical stimuli (red arrows) were delivered at the start of every fourth frame (every fifth frame for some experiments). (*B*) Raster plot of simple-cell responses to combined electrical and white-noise visual stimulation. Electrical stimuli were applied at time 0, as shown in *A*. Each electrical stimulus (200 μA) coincided with the start of every fourth visual frame (total frames: 32,768); therefore, 8,192 electrical stimuli were presented over the course of ≈16 min. In this example, only 4 of 4,838 spikes occurred later than ≈2 ms after the electrical stimulus. (*C*) Raster plot of responses to white-noise visual stimulation alone. Without electrical stimulation, spikes (1,298 total) occurred at more evenly distributed times. In this example there were more spikes in the stimulated condition than in the control, but this was not always the case.

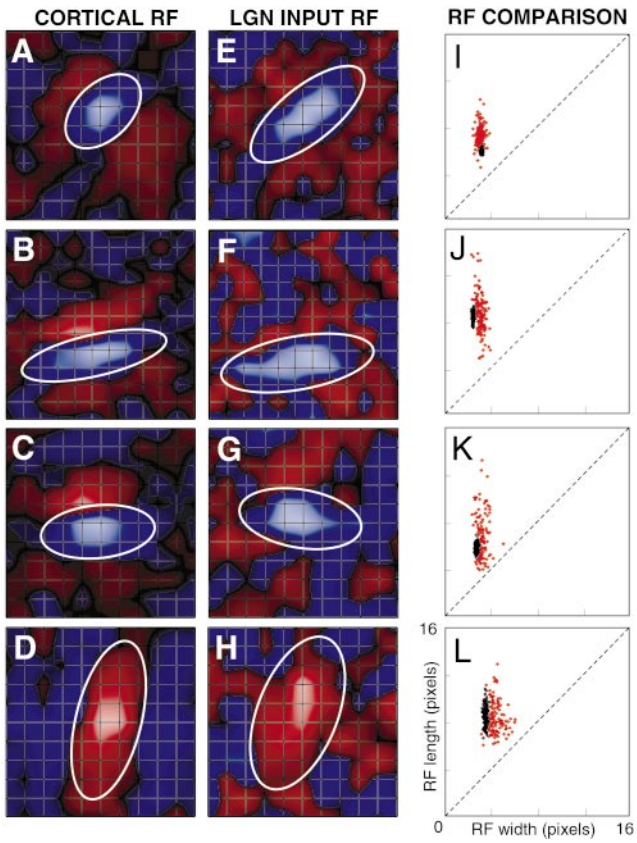

Fig. 4. Spatial receptive fields of cortical layer 4 simple cells and of their thalamic input. (*A–D*) Receptive fields of four simple cells under control conditions. *Off* subfields are shown in blue, and *on* subfields are shown in red. Gridlines show individual stimulus pixels (0.4–0.6°). The elongated primary subfield of each cortical cell was fitted with a 2D Gaussian (shown as ellipses at 1.75σ). (*E–H*) Receptive field of the thalamic input for the four cells shown in *A–D*, as obtained with combined visual and electrical stimulation. In all four cases, the primary subfield remained elongated. Stimulation currents for *E*, *F*, *G*, and *H* were 100, 200, 225, and 200 μA, respectively. (*I–L*) Primary subfield length vs. width for simple cells (black) and their thalamic input (red) for each of the four cases shown in *A–H*. Each point corresponds to parameters derived from one iteration of our error analysis (see *Materials and Methods*). All values lie above the diagonal line of unit slope, indicating that the receptive fields of the cortical neurons and their thalamic inputs were both significantly elongated (Wilcoxon signed rank tests, $P < 0.0001$ in all cases).

(118 or 147 ms) were phase locked to the start of that visual stimulus frame (see Fig. 3 *A* and *B*). For some cells, we performed a similar analysis during sine grating visual stimulation, in which repetitive electrical pulses were applied every 90 ms (eight times over three stimulus cycles, where each visual stimulus grating cycle lasted 240 ms) so that electrical stimuli coincided with 8 unique phases of a single cycle of the grating stimulus (see Fig. 2*B*).

Data Acquisition. Neural signals were bandpass filtered at 0.3–5 KHz and digitized at 20 KHz (Cambridge Electronic Design, Power 1401). Cortical data were analyzed to confirm single-unit isolation via waveform template analysis, cluster separation, and the presence of absolute refractory periods in the spike trains. With one exception, the largest unit recorded with the cortical electrode was used for receptive-field analysis. In one control experiment, in which we assessed the extent of electrically evoked cortical silencing, we analyzed multiunit data (up to three unique spike waveforms per electrode) from layers 4 and 6.

Gaussian Fitting and Error Analysis. To compare the normal cortical receptive field with the receptive field of the thalamic input, we first considered the primary (strongest) subfield. The spatial receptive field was defined as the average stimulus that preceded each spike in the range 29–89 ms (stimulus frames 2 and 3; in one case, only frame 3 was used). The lengths and widths of the primary subfields were quantified by fitting the spatial receptive fields, RF(X,Y), to elliptical Gaussians,

$$A \cdot e^{-\left[\frac{(x-x_c)^2}{\sigma_x^2}+\frac{(y-y_c)^2}{\sigma_y^2}\right]},$$

where A is the amplitude, x_c and y_c are positions of the center, and σ_x and σ_y are standard deviations. The coordinates, x and y, are obtained by rotating the stimulus coordinates, X and Y, by an angle determined by the fitting procedure.

We estimated the reliability of the parameters derived from the Gaussian fit with the following error analysis. First, the noise in our receptive field measurements was estimated from the average stimulus that preceded each spike by delays longer than the visual response (from 13–16 stimulus frames, or ≈400–500 ms). Then, to assess the sensitivity of the Gaussian fits to noise (see Fig. 4 *I–L*), we added randomly chosen pixel values from our noise estimates (frames 13–16) to the measured receptive fields (frames 2 and 3, see previous paragraph). This procedure was repeated 128 times to produce 128 unique elliptical fits of the primary subfield.

Secondary (flanking) subfields were easily detected in normal cortical receptive fields, but they were considerably harder to

discern in the receptive fields of the thalamic inputs, in part because of the increased baseline noise. To quantify changes in the ratio of the secondary subfields to the peak subfield, we masked these regions as follows. Over the ellipse used to fit the peak subfield (drawn at 1.75 σ), we drew a concentric ellipse that was three times wider (see Fig. 6, which is published as supporting information on the PNAS web site, www.pnas.org). The ratio of the flanking subfields to the primary subfield was calculated as the difference between the sum of the pixel values in these two ellipses divided by the sum of the pixel values in the peak subfield.

Results

Combined visual and electrical stimulation experiments were performed in 15 layer 4 simple cells along the medial bank of striate cortex. All 15 cells were well-isolated units that received monosynaptic input from the LGN (latency range: 1.8–2.4 ms; mean latency across all cells: 2.12 ms). Cells for which we could not evoke monosynaptic spikes were not included in our data set.

Modulating the Probability of Electrically Evoked Spikes During Visual Grating Stimuli. In the 15 simple cells that received monosynaptic input from the LGN, electrical stimuli were applied during one or more phases of the drifting sinusoidal grating visual stimulus. By first applying the electrical stimuli near the peak of the visual response, we could test the efficacy of a range of stimulation currents with high sensitivity. Efficacy was defined as the fraction (or percent) of stimulation trials that evoked spikes with monosynaptic (1.8–2.4 ms) latency. We found that 5 μA of stimulation current produced a modest efficacy of evoking cortical spikes compared with the baseline from the unstimulated control (Fig. 2*A*). Higher currents (50–500 μA) produced a progressively higher probability of monosynaptic spikes and correspondingly longer-lasting silencing of cortical discharge (50–200 ms; Fig. 2*A*).

Once we found a stimulation current that would likely suppress the simple cell's spikes (except for spikes immediately after the electrical stimulus), for 4 of 15 cells we applied this single current at eight different phases of the visual stimulus at a rate of 11 Hz. Even though the stimulation current was fixed, the probability of evoking a monosynaptic spike depended strongly on its timing relative to the visual stimulus (Fig. 2*B*) for all four cells tested. For the cell whose responses are shown in Fig. 2*B*, only monosynaptic spikes were evoked during this repetitive electrical stimulation paradigm; at all other times between electrical pulses, there were no cortical spikes (data not shown).

As discussed in the introduction, repetitive electrical stimulation served double duty (see Fig. 1*B*). First, electrical stimuli produced a long-lasting intracortical inhibition that suppressed all spiking activity between stimuli. Second, they probed the subthreshold cortical membrane potential at the time of the electrical stimulus. Because cortical spiking was inhibited in the 90 ms between electrical stimuli (three-eighths of the repeat period of the visual stimulus, see *Materials and Methods*), all remaining visual input must have derived from the LGN (assuming that other cells in the cortex were similarly silenced, see Fig. 7, which is published as supporting information on the PNAS web site). The suprathreshold visual response from the control experiment (blue histogram in Fig. 2*B*) was narrower than the inferred subthreshold thalamocortical visual input from the electrical stimulation experiment (red curve in Fig. 2*B*). This finding is consistent with previous studies in which direct intracellular measurements of sub- and suprathreshold visual responses were made (11). Further, the control visual response occurred during the rising phase of the monosynaptic response (Fig. 2*B*), consistent with the fact that spikes typically occur on the rising phase of the membrane potential rather than the falling phase (12).

Combined Visual White Noise and Repetitive Electrical Stimulation Isolate the Receptive Field of the Thalamic Input to Individual Cortical Cells. To examine the spatial receptive field of the thalamic input, we used white-noise visual stimuli (see *Materials and Methods*). The advantage of using white noise is that it is uncorrelated from one stimulus frame to the next, unlike the grating stimulus. In particular, the visual stimuli in the interval between two electrical impulses are uncorrelated with all previous visual stimuli.

During white-noise visual stimulation alone, the average firing rate of our sample of 15 cortical cells ranged from 0.34 to 7.25 Hz (mean: 2.35 Hz). In 11 of these 15 cells, we combined electrical stimulation of the LGN with white-noise visual stimuli. The white-noise visual stimulus was updated every 29.4 ms, and electrical stimuli were applied at the start of every fourth or fifth visual stimulus frame (Fig. 3*A*). Repetitive electrical stimulation under these conditions produced monosynaptic spikes with variable efficacy and subsequent inhibition until the next electrical stimulus 118 ms later (147 ms in some experiments). A raster plot of the responses from such an experiment is shown in Fig. 3*B*. Electrical stimuli were applied at time zero. Throughout the experiment, 200-μA stimulation spared electrically evoked spikes and effectively suppressed all other (visually evoked) spiking of this cortical cell (compare with the control in Fig. 3*C*). In this example, monosynaptic spikes were evoked with 59% efficacy. For the 11 cells tested, the efficacy ranged from 1% to 100% (17 $\pm$ 32%, mean $\pm$ SD).

In three cases, the inhibition of cortical firing between electrical stimuli took 10–100 s to develop. The data presented and analyzed in this paper were not taken from this initial warm-up period, whose mechanism was not explored. Receptive fields from two of these three cases are plotted in Fig. 4 *E* and *G*.

Spatial Receptive Field Geometry: Unstimulated Control vs. Isolated Thalamic Input. For 6 of 11 simple cells studied with the above protocol, we were able to map simple receptive fields first without electrical stimulation and then under conditions in which electrical stimulation revealed their isolated thalamic input (see *Controls: Retinotopic Overlap and Spatial Extent of Cortical Silencing*). Simple cells in layer 4 typically have two or three clearly defined *on* and *off* subfields (Fig. 4 *A–D*). The mean aspect ratio (length to width) of the primary subfield was 2.7 $\pm$ 0.8 (mean $\pm$ SD, $n = 6$), consistent with a previous report (2). The mean aspect ratio of the corresponding subfields from the isolated thalamic input was 2.4 $\pm$ 0.3 (mean $\pm$ SD), suggesting that the thalamic input provides an elongated input to cortical simple cells (see Fig. 4 *E–H*). The average aspect ratio of the primary subfield across all cells tested was not significantly different between the two conditions (control vs. electrical stimulation, $P > 0.05$, Mann–Whitney *U* test). Error analysis of the individual estimates of the length and width of the primary subfield (see *Materials and Methods*) showed that the thalamic input was significantly elongated in all cases (Fig. 4 *I–L*; Wilcoxon Signed Rank test, $P < 0.001$ in each case).

Although the primary subfields of the thalamic input closely matched those of the unstimulated control, the secondary flanking subfields were qualitatively weaker, particularly in two cases (compare Fig. 4 *B* and *F*, and *D* and *H*). We quantified the relative strength of the flanking subfields by taking the ratio of their summed strength to that of the primary subfield (see *Materials and Methods* and Fig. 6). In the four cases shown in Fig. 4, electrical stimulation resulted in a reduction of the relative strength of the secondary flanking subfields by 33%, 79%, 32%, and 86%, respectively. Across all six cases, the ratio of the flanking subfields to the peak subfield (see *Materials and Methods*) was significantly weaker ($P < 0.05$, Mann–Whitney *U* test).

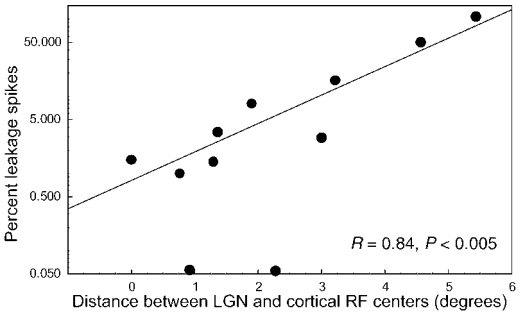

Fig. 5. Extent of electrically evoked silencing depends on the retinotopic separation of the LGN stimulation and cortical recording sites. The retinotopic position of each site was defined by taking the absolute value of the receptive field (single-unit in cortex, multiunit in LGN), thresholding, and then calculating the center of mass. The greater the receptive field separation, the more leakage or unsuppressed spikes detected in the 89-ms window preceding each electrical stimulus (as a fraction of the control condition). The two recordings with absolute suppression (zero leakage spikes) were plotted at the arbitrary level of 0.01% leakage and were not included in the regression.

Controls: Retinotopic Overlap and Spatial Extent of Cortical Silencing. The logic of our experiments requires that cortical silencing be extensive in both time and space. In time, it is necessary that there are no cortical spikes between successive electrical stimuli, so that the only visual input to a cortical neuron must come from the LGN. It might be argued that the visual responses probed by one electrical stimulus could influence the responses to the next electrical stimulus. With white noise, however, the visual stimuli in each successive interval are uncorrelated, so persistent influences of electrical stimuli cannot confound our measurements of spatial receptive fields. It is worth noting that the spatial receptive fields we report were derived from stimulus frames presented 29–89 ms before the electrically evoked spike (see *Materials and Methods*), but the electrical stimuli are spaced by 118 or 147 ms.

In space, it is necessary to silence the entire population of cortical neurons that might project to the neuron being studied. To ensure that this was the case, we analyzed the degree of silencing as a function of the retinotopic distance between the cortical receptive field and the LGN stimulation site.

When retinotopic separation distances were large (>3°), we could not find stimulation parameters (current and frequency) such that there was both >95% inhibition of the visual response and also a modest probability ($P \approx$ 1–60%) of evoking monosynaptic spikes with each stimulation pulse. Even with high stimulation currents (e.g., 500 μA), cortical spikes were not suppressed for the full interstimulus interval and leakage spikes were detected (defined as spikes occurring in the 89 ms, or three stimulus frames, preceding each electrical pulse). If the cortex was silenced for only the first 40–60 ms of the interstimulus interval, then a rebound discharge (activity even greater than detected in control conditions) was observed (see Fig. 8, which is published as supporting information on the PNAS web site).

The fraction of leakage (unsuppressed) cortical spikes was directly related to the retinotopic separation of the LGN stimulation site and the cortical simple cell receptive field (Fig. 5). Most importantly, if the retinotopic separation between geniculate and cortical receptive fields was less than 1.5° of visual angle (as was the case for all four cells in Fig. 4), then >95% inhibition was attained by using 200–225 μA electrical stimulation (100 μA used in one case: see receptive field in Fig. 4*A* and raw data in Fig. 8*A*). Within 5° of area centralis, the maximum eccentricity of the receptive fields we studied, 1.5° of visual angle corresponds to 1.5–2.6 mm across the cortical surface (13).

In total, 7 of 11 cells were effectively silenced to >95% (our criterion level for effective silencing, as in ref. 4). In the other 4 of 11 cases, a significant number of leakage spikes were detected, suggesting that the thalamic input was not well isolated. We mapped the receptive field of the isolated thalamic input in only six of seven of cases with >95% silencing. In the remaining example, the efficacy of electrical stimulation was 100%. A receptive field map was therefore not obtained because the visual stimulus could not modulate the efficacy of electrical stimulation.

The above data suggest that when the simple cell receptive field overlapped the receptive field of the LGN stimulation site to within 1.5° (or 1.5–2.6 mm across the cortical surface), nearby cortical cells are also likely to be effectively silenced. These other cortical cells are therefore unlikely to contribute to the receptive fields we mapped during electrical stimulation. To gain further confidence that we had effectively silenced the cortical input to the layer 4 cells that we were studying, we made parallel electrode penetrations in the two layers (layers 4 and 6) that provide synaptic input onto layer 4 cells (see Fig. 7). We collected single and multiunit activity from four sites in layer 4 (spanning a distance of ≈1 mm) and one retinotopically matched site from layer 6. During combined white-noise visual stimulation and 225 μA LGN electrical stimulation, leakage spikes in cortical layer 4 were suppressed by an average of 97% (compared with the unstimulated control). In layer 6, 200 μA suppressed leakage spikes by 100%. These values are for the largest amplitude single-unit spike recorded at each site, for which the peristimulus time histogram (PSTH) and raster plot are shown in Fig. 7. Multiunit activity (up to three smaller spikes, see *Materials and Methods*) was also suppressed by >95% in layers 4 and 6 (data not shown).

It might be argued that cortical activity outside the silenced region could affect the receptive fields we measured during repetitive stimulation. We believe this is very unlikely for the following reason. Unlike the long-range horizontal connections in cortical layer 2 of 3, both layer 4 and 6 neurons have spatially restricted axonal arbors (maximum width ≈1 mm) in layer 4 (14, 15). Thus, if both layer 4 and layer 6 are silenced nearby (see Fig. 7), there is no pathway through which cortical activity outside the silenced region might be propagated to the layer 4 neurons under study.

Discussion

We combined visual and electrical stimulation with extracellular single-unit recording to estimate the spatial profile of the afferent synaptic input to individual cortical simple cells. Provided that the retinotopic site of LGN electrical stimulation matched the cortical recording site to within ≈2°, intracortical spiking could be silenced while sparing the electrically evoked monosynaptic response. Modulation of the electrically evoked response by ongoing visual stimuli provided a measure of the subthreshold visual LGN input arriving at cortical simple cells. Repetitive electrical stimulation of the LGN afferents during presentation of white-noise visual stimuli could therefore be used to map the receptive field of the thalamic inputs. We found that the receptive field of this isolated thalamic input was elongated, with aspect ratios comparable to the aspect ratios of the original receptive fields. Secondary (or flanking) subfields of the thalamic input, however, were weaker than those of the original receptive fields.

Our stimulation technique is versatile enough to address the extent to which the thalamic input might contribute to other aspects of the cortical receptive field, such as contrast gain control and direction selectivity. For instance, if contrast gain control disappeared in the silenced cortex, it would suggest that the cortical circuit is important in producing this property. Positive results such as the elongation of thalamic input reported here, however, do not preclude a role of the cortical circuit in refining the cortical receptive field, or in amplifying the thalamic

input. If, for instance, the orientation selectivity of the thalamic input was similar to that in the intact cortex (as in ref. 4), the cortical circuit might make that property more robust (16–20).

Our extracellular recordings did not allow us to distinguish unequivocally between excitatory and inhibitory cells in layer 4, both of which typically have simple receptive fields (21, 22). Swadlow's group, however, has shown that electrical stimulation of thalamic afferents in the rabbit somatosensory and visual systems may reveal whether monosynaptically activated cells are inhibitory (23, 24). In particular, only fast spiking inhibitory cells fire multiple action potentials in responses to an electrical stimulus, and they also have the shortest latencies (24). Three of our 15 cortical cells that received monosynaptic input from the LGN (and 2 of 7 that were >95% silenced with repetitive stimulation) satisfied two of Swadlow's criteria for identifying inhibitory cells (see Figs. 7*C* and 8*A*). This finding suggests that our stimulation protocol likely inhibited both excitatory and inhibitory layer 4 simple cells and that the thalamus provides an oriented input to both classes of cells.

The rich inhibitory circuitry in the LGN (25) suggests that electrical stimulation of the LGN presumably causes local inhibition as well as inhibition in the cortex (H. A. Swadlow, personal communication). At one extreme, if inhibition in the geniculate were equal or longer in duration than in cortex, visual input to cortex would be silenced in our protocols so that electrically evoked spikes would not have a receptive field. The fact that we can map receptive fields when the cortex is effectively silenced (see Fig. 4) implies that the LGN is not silenced during the entire 120–150 ms interstimulus interval. Indeed, electrical stimulation of the optic chiasm and intracellular recording from relay cells in the thalamus *in vivo* show that 86% of thalamic cells produce inhibitory postsynaptic potentials that completely recover within 60 ms (26).

It is important to point out that the neurons being stimulated need not have been the same as the inputs whose functional role was being studied. Here we stimulated in the LGN to study the isolated influence of the LGN on layer 4 simple cells. As noted above, however, the key point was that electrical stimulation met two criteria: (*i*) to evoke monosynaptic spikes with some probability less than 100%, so that subthreshold activity could modulate that probability; and (*ii*) to cause prolonged and widespread inhibition, so that nonthalamic visual inputs to layer 4 neurons (in particular nearby layer 4 and layer 6 neurons) were silenced in the period between electrical stimuli. In principle, stimulation in other regions that provide excitatory input to layer 4 might have achieved the same result, such as layer 4 itself or layer 6, although in practice it might not be possible to find stimulation parameters that satisfy both criteria.

In conclusion, combining electrical and visual stimulation with extracellular recording is an effective tool for studying the selectivity and organization of feed-forward inputs to cortical cells, albeit indirectly. Our results suggest that the spatial receptive field of the thalamic input is significantly elongated and has an aspect ratio comparable to that of the primary subfield of normal cortical simple cells. This provides further, independent evidence that the shape of a simple cell's receptive field is imposed by connections from a specific subset of the local LGN afferents (1, 27).

We thank Sasha Vagodny for technical assistance with surgery and histology. We thank Marc Sommer, Daniel Butts, and Patrick Kanold for valuable discussions. This work was supported by National Institutes of Health Grants R01 EY10115, R01 NS41000, and P30 12196, the Dana/Mahoney Fellowship Fund, and the Lefler Fund.

1. Reid, R. C. & Alonso, J. M. (1995) *Nature* **378,** 281–284.
2. Alonso, J. M., Usrey, W. M. & Reid, R. C. (2001) *J. Neurosci.* **21,** 4002–4015.
3. Ferster, D., Chung, S. & Wheat, H. (1996) *Nature* **380,** 249–253.
4. Chung, S. & Ferster, D. (1998) *Neuron* **20,** 1177–1189.
5. Berman, N. J., Douglas, R. J., Martin, K. A. & Whitteridge, D. (1991) *J. Physiol. (London)* **440,** 697–722.
6. Douglas, R. J. & Martin, K. A. (1991) *J. Physiol. (London)* **440,** 735–769.
7. Kara, P., Reinagel, P. & Reid, R. C. (2000) *Neuron* **27,** 635–646.
8. Merrill, E. G. & Ainsworth, A. (1972) *Med. Biol. Eng.* **10,** 662–672.
9. Ferster, D. & Lindstrom, S. (1983) *J. Physiol. (London)* **342,** 181–215.
10. Reid, R. C., Victor, J. D. & Shapley, R. M. (1997) *Visual Neurosci.* **14,** 1015–1027.
11. Carandini, M. & Ferster, D. (2000) *J. Neurosci.* **20,** 470–484.
12. Azouz, R. & Gray, C. M. (2000) *Proc. Natl. Acad. Sci. USA* **97,** 8110–8115.
13. Tusa, R. J., Palmer, L. A. & Rosenquist, A. C. (1978) *J. Comp. Neurol.* **177,** 213–235.
14. Martin, K. A. & Whitteridge, D. (1984) *J. Physiol. (London)* **353,** 463–504.
15. Katz, L. C. (1984) *J. Neurosci.* **7,** 1223–1249.
16. Somers, D. C., Nelson, S. B., Sur, M. (1995) *J. Neurosci.* **15,** 5448–5465.
17. Douglas, R. J., Koch, C., Mahowald, M., Martin, K. A. & Suarez, H. H. (1995) *Science* **269,** 981–985.
18. Sompolinsky, H. & Shapley, R. (1997) *Curr. Opin. Neurobiol.* **7,** 514–522.
19. Ferster, D. & Miller, K. D. (2000) *Annu. Rev. Neurosci.* **23,** 441–471.
20. Sharon, D. & Grinvald, A. (2002) *Science* **295,** 512–515.
21. Martin, K. A., Somogi, P. & Whitteridge, D. (1983) *Exp. Brain. Res.* **50,** 193–200.
22. Azouz, R., Gray, C. M., Nowak, L. G. & McCormick, D. A. (1997) *Cereb. Cortex* **7,** 534–545.
23. Swadlow, H. A. (1988) *J. Neurophysiol.* **59,** 1162–1187.
24. Swadlow, H. A., Beloozerova, I. N. & Sirota, M. G. (1998) *J. Neurophysiol.* **79,** 567–582.
25. Sherman, S. M. & Koch, C. (1990). in *The Synaptic Organization of the Brain,* ed. Shepherd, G. (Oxford Univ. Press, New York), pp. 246–278.
26. Bloomfield, S. A. & Sherman, S. M. (1988) *J. Neurophysiol.* **60,** 1924–1945.
27. Hubel, D. H. & Wiesel, T. N. (1962) *J. Physiol. (London)* **160,** 106–154.